

Second-Harmonic Imaging of Collagen

Guy Cox and Eleanor Kable

Summary

Molecules that have no center of symmetry are able to convert light to its second harmonic, at twice the frequency and half the wavelength. This only happens with any efficiency at very high light intensities such as are given by a pulsed laser, and because the efficiency of the process depends on the square of the intensity, it will be focal plane selective in exactly the same way as two-photon excitation of fluorescence. Because of its unusual molecular structure and its high degree of crystallinity, collagen is, by far, the strongest source of second harmonics in animal tissue. Because collagen is also the most important structural protein in the mammalian body, this provides a very useful imaging tool for studying its distribution. No energy is lost in second-harmonic imaging, so the image will not fade, and because it is at a shorter wavelength than can be excited by two-photon fluorescence, it can be separated easily from multiple fluorescent probes. It is already proving useful in imaging collagen with high sensitivity in various tissues, including cirrhotic liver, normal and carious teeth, and surgical repair of tendons.

Key Words: Collagen; second harmonic; structural proteins; biological imaging; 3D imaging; non-linear microscopy; matrix.

1. Introduction

1.1. Second-Harmonic Generation

Theodore Maiman won a much publicized race to make a working laser when he built a pulsed ruby laser in 1960. This was the world's first laser and it produced pulses of deep red (697 nm) light, just within the visible range. Almost immediately, it was found that shining pulses of ruby laser light through a quartz crystal produced near-ultraviolet light at 348 nm, the second harmonic of the original light (*I*).

Second-harmonic generation (SHG) takes place when the electric field of the exciting light is sufficiently strong to deform a molecule. If the molecule is not symmetrical, the resulting anisotropy creates an oscillating field at twice the

frequency, the second harmonic (2). This means that the ability to generate second harmonics is peculiar to molecules that are not centrosymmetric. SHG will also take place at interfaces where there is a huge difference in refractive index, such as metal surfaces. For a more technical description, *see* **Note 1**.

The resulting beam of light at twice the frequency/half the wavelength usually travels in the same direction as the incident beam and in phase with it, although it commonly has a different plane of polarization. Different samples and illumination conditions will modify this behavior; the whole question of beam propagation is discussed in more detail in **Subheadings 2.3.** and **3.1**. Crystals of nonsymmetric molecules such as potassium deuterium hydrogen phosphate are very effective generators of second harmonics, and particularly when the angle of the crystal lattice is carefully matched to the incoming beam, they can give extremely high second-harmonic yields. The production of suitable crystals (potassium, cesium, or rubidium titanyl phosphate or arsenate are other common examples) is an important industry; and the crystals are in everyday use as frequency doublers in the laser industry—even humble items such as green laser pointers contain a frequency-doubling crystal.

Second-harmonic generation was first used in microscopy as long ago as 1974 (3) (*see* **Note 2**), but the more practically useful technique of scanned second-harmonic microscopy was first achieved 4 yr later, by Gannaway and Sheppard (4), using a continuous-wave laser. All modern applications stem from this work. As they pointed out, in the scanning mode the image is focal plane selective because the signal depends on the square of the incident beam power. It is, thus, effectively equivalent in imaging properties to confocal microscopy and two-photon fluorescence; the fact that it is coherent rather than incoherent does cause small differences, but they are only of theoretical interest so far as biological applications are concerned. Scanning the beam across the sample means that high intensities only have to be present in a very small region at any one time, but, even so, the continuous-wave laser used by Gannaway and Sheppard necessitated power densities at the sample that could not be tolerated by biological specimens. It was clear even then that pulsed lasers would make the technique more practicable, and the introduction of second-harmonic microscopy as a practical technique had to await the availability of pulsed lasers with very short pulse lengths. These now offer very high instantaneous powers in conjunction with low total power averaged over time, at a repetition rate fast enough not to restrict scan speed.

Second-harmonic-generation microscopy has many features in common with two-photon fluorescence (TPF) microscopy, and the hardware required is very similar, but there are some key differences (summarized in **Table 1**). Fluorescence always involves some loss of energy in the sample, and the fact that electrons are raised to excited states means that bleaching is inevitable.

Table 1
Comparison of SHG and TPF

SHG	TPF
Exactly double the original frequency	Spectrum of frequencies less than two times the original
Largely frequency independent	Strongly frequency dependent
Virtually instantaneous, approx 1 fs	Lifetime in nanoseconds
Propagated forward	Propagated in all directions
Coherent (in phase with exciting light)	Incoherent
No energy loss or damage	Always energy loss and associated damage
Requires short laser pulses	Requires short laser pulses

SHG dissipates no energy in the sample and there is no excitation or bleaching. Of course, that does not imply that no damage can occur; there are several mechanisms through which intense laser pulses can damage the sample, but these are totally independent of the imaging process.

Serious biological use of SHG microscopy has been a recent phenomenon, with few papers dated prior to 2001. Gauderon et al. (2) were able to image the DNA of polytene chromosomes of *Drosophila*. Campagnola et al. (5) applied the known SHG properties of styryl potentiometric dyes to the microscope, continuing from earlier work in which these properties had been investigated in the cuvet. They also imaged collagen and other structural proteins in a variety of tissues at resolutions of up to 1 μm (5,6). Membranes have been labeled with second-harmonic generating dyes, providing a sensitive probe of membrane separation (7,8).

1.2. Collagen and SHG

Individual noncentrosymmetric molecules will generate a second-harmonic signal, but molecules arranged in a crystalline array will give a very much stronger response. Hence, any biological material that is both crystalline and noncentrosymmetric is likely to be suitable for SHG microscopy. Furthermore, SHG microscopy of such materials should be capable of providing information about orientation and crystallinity, as well as morphology.

Collagen is the most important extracellular structural protein of the vertebrate body, making up around 6% of the body mass, mainly in bone, cartilage, skin, interstitial tissues, and basal laminae. The collagen molecule is nonsymmetric and is arranged in a triple helix (9). There are many different forms of collagen, coded separately in the genome. Minor amino acid changes affect the final conformation and, therefore, give the different collagen types different functions in the living organism. Four types (I, II, III, and V) form fibrils, type

IV forms sheets in basal laminae, and types VI and IX act as links, binding fibrillar collagen to other cell components. Type I, in particular, is highly crystalline and is very important as a structural component of the skeleton, cartilage, and soft tissue.

This unusual structure makes type I collagen an effective generator of second harmonics, a fact that has been appreciated for over 20 yr (*10*). The signal is, to a large extent, wavelength independent over a wide range of wavelengths in the infrared region (*11,12*). Furthermore, it is possible from this signal to determine the polarity of the collagen helix (*13*). Differences in signal between normal and experimentally damaged collagen have also been reported (*14*), raising the hope that pathological changes might be detected. Very recently, spectral changes in the second-harmonic signal from normal and cancerous tissue have been described, opening up a possibility that it might become a useful diagnostic tool in oncology (*15*). We have shown that SHG can be an exquisitely sensitive tool for detecting and imaging collagen at high resolution, with diffraction-limited resolution (sub-300 nm) easily achievable (*12,16*). There seems to be the potential to distinguish between different collagen types, with highly crystalline type I collagen giving a much stronger second-harmonic signal than type III, even though both stain identically with collagen-specific dyes (*12*).

2. A Microscope for SHG Imaging

The basic requirements for SHG microscopy are those for TPF microscopy: a scanning microscope (usually a confocal microscope, although confocal optics are irrelevant) coupled to a pulsed infrared laser. However, the different nature of signal generation in SHG microscopy means that some simple and straightforward modifications to a normal multiphoton microscope will be needed.

2.1. The Laser

A pulsed titanium–sapphire (Ti-S) laser is the normal choice, although neodymium yttrium aluminium garnet (Nd YAG) lasers have been used (*11*), and, in principle, other lasers such as chromium forsterite are possible and might come into wider use in the future. Because SHG depends on the square of the flux density, shorter pulses will mean a substantial reduction in the average power required. Therefore, in principle at least, a “femtosecond” Ti-S laser (typically delivering 100- to 200-fs pulses) will usually be preferred over a “picosecond” version, which delivers 1- to 2-ps pulses.

However, to gain the full benefit of short pulses, it is essential that they remain short. Light travels approx 30 μm during a 100-fs laser pulse, so the pulse will contain fewer than 40 waves at 800 nm. With such a small number

of waves in a pulse, the wavelength cannot be specified with great precision and, consequently, there will be a range of wavelengths present in a Gaussian distribution with a full width at half-maximum (FWHM) range of about 2 nm. This makes no difference in terms of biological imaging, as the spread is narrower than the band passed by current detection systems, whether filter based or spectro-metric. It is also trivial in terms of TPF excitation. However, it is very much wider than the completely monochromatic light produced by a continuous-wave laser. There is an important practical consequence of this wavelength spread: It will broaden the pulse if it travels through a dense medium such as glass. All glass has dispersion; that is, its refractive index is wavelength dependent, so that longer wavelengths travel more slowly than shorter ones. In a very short laser pulse, therefore, the different wavelengths will travel at different speeds and the pulse will broaden. Longer pulses have a much smaller wavelength spread, so they will not be affected to the same extent; in practical terms, pulse broadening is only a problem in the femtosecond region.

A consequence of this is that the laser needs to be directly coupled to the microscope; transmitting the light through an optical fibre will broaden the pulse to an unacceptable extent (*see Note 3*). Any additional optical elements in the beam path—even such useful items as beam expanders—will lengthen the pulse, as will objective lenses; so the less glass in the objective, the better. This implies that there is little point in using complex lenses such as apochromats, especially because color correction is irrelevant (only one wavelength has to be brought to a focus). Fluorite lenses typically offer comparable numerical apertures with many fewer elements, and because their basis is the low-dispersion mineral fluorite (calcium fluoride), pulse broadening is minimal.

Femtosecond Ti-S lasers fall into three categories:

1. Fully tuneable between 700 and 1000 nm. These lasers typically have a range of manual adjustments that need attention in normal operation, and more than one set of optical components might be needed to obtain the widest tuning range, although 700 to 950 nm or 750 to 1000 nm are typically now available with a single optics set.
2. Tunable over a limited range, but fully automated so that no external adjustments need to be made. The tunable range available with these is increasing rapidly, and although fully tuneable lasers still offer a wider range at the time of writing (June 2003), the automated models are now very close to them in performance and might well match them before long.
3. Fixed wavelength, commonly 800 nm.

Fixed-wavelength lasers are not very suitable—unless set to a rather longer wavelength than 800 nm—because detection of the second harmonic at 400 nm is often blocked or attenuated by other optical elements in the microscope. Automated lasers are probably now the most effective solutions, unless other

usage requirements dictate a wider tuning range. Because the SHG signal from collagen shows little wavelength dependence within the tuning range of a Ti-S laser, wider range lasers do offer the facility of optimizing laser wavelength for multiphoton fluorescence excitation without compromising SHG detection. In particular, effective two-photon excitation of many members of the GFP (green fluorescent protein) family requires long wavelengths that lie beyond the range of automated lasers (*see Note 4*).

Tunable lasers are tuned by moving a birefringent element, but this, in turn, will require adjustments to a prism to compensate group velocity dispersion—ensuring that all wavelengths remain together within the laser cavity—and there will also be alignments to mirrors and the slit that acts to impose mode locking on the pulses. Hence, a fully tunable laser requires not only an investment in technology but also an investment in expertise to keep it correctly adjusted.

2.2. Ancillaries

The coupling system to the microscope, whether lab built or supplied by the microscope maker, will need to divert part of the beam to diagnostic equipment. A spectrum analyzer is the most useful ancillary, showing not only the actual wavelength tuned but also the spread of wavelengths present. This is a very effective visual indication of the pulse length, and software is available that will compute an estimated pulse length from the spread, although this does depend on some assumptions about the pulse shape. An autocorrelator will give a more precise measure of the pulse length, but is a fiddly and complex instrument to use, although, again, rapid strides are being made in improving usability for the biologist. Recently, models have been produced that provide a remote head to measure the actual pulse width emerging from the objective. A power meter is also valuable, even if the diagnostics built into the laser itself gives a power reading, because an independent power meter can pick up losses further along the beam path. Often, a decline in power will be a useful warning that either the laser is not perfectly aligned or that the internal optics are in need of cleaning.

As discussed in **Subheading 2.1.**, the beam delivery to the microscope must be direct, not through an optical fiber. Normally, therefore, the microscope and laser will both be rigidly mounted to an optical table. Microscope manufacturers might have some degree of standardization in their hardware, but these systems are still largely custom installations, so the user will have a fair degree of choice. Points to consider include the following:

1. The range and convenience of alignment of the beam, because the pointing stability of Ti-S lasers is often rather worse than is normal for continuous-wave lasers.
2. The control over beam power. Although neutral density filters will provide attenuation, an electronic control such as a Pockel Cell or electro-optic modulator (EOM) will allow beam blanking on flyback (thus reducing the total beam exposure of the sample) as well as patterned irradiation.

3. The efficiency of the total throughput. Often much light is lost before it even reaches the microscope. Many partial beam splitters (used to divert part of the beam to diagnostic equipment) have a surprisingly high absorbance in the 700- to 900-nm range. A piece of plain, uncoated glass is often at least as effective as a custom beam splitter. If much power is disappearing, it is worth carrying out an audit with a power meter to see where the losses are.

2.3. The Microscope

Whereas second harmonic light is generally propagated forward, geometric considerations (the Gouy phase shift in a focused spot) might mean that much of the flux emanating from the scanning spot is in the off-axis directions (7,8). Therefore, for effective collection, the condenser lens must have a numerical aperture (NA) equal to or larger than that of the objective. An oil-immersion condenser is a necessity. Equally important is that Köhler illumination be set up with scrupulous precision. Without this, a large proportion of the second-harmonic light will never reach the detector. Having a totally immersed system also reduces the amount of stray room light that can enter, an important consideration with any form of nondescanned detector.

Although they provide geometrically perfect focusing, galvanometer stage movements do not function well in this environment. The combination of short working distances and viscous drag from the immersion media impede the free motion of the stage, so that it often fails to follow the instructions given by the controlling computer. Even though, in theory, moving the sample between a stationary objective and condenser achieves optical perfection, it is preferable in practice to focusing with the nosepiece; a high precision is achieved with electronic or piezo-driven nosepieces. Generally, the precision with which a series can be collected will be very high, but the reproducibility will be less so; thus, there might be visible errors in returning to a given focal plane.

Unless one wishes to work in total darkness, every attempt should be made to prevent room light from reaching any of the nondescanned detectors. **Figure 1** shows the Leica screening arrangements as fitted to our microscope. Around the condenser, we have a large (10 cm) matt-black disk, which serves a dual function in excluding room light as well as safeguarding against accidental laser exposure. From the condenser to the lamp housing is a close-fitting matt black telescopic tube, which keeps out all room light above the condenser.

The slider that blocks off the wide-field epifluorescence illuminator (high-pressure mercury or argon arc lamp) often passes a surprisingly large amount of light when closed. Although this is not noticeable in conventional epifluorescence microscopy, it can interfere substantially with two-photon or second-harmonic detection. Because it is often not convenient to turn off the mercury lamp, a blanking plate should be made up to fit in the lamp housing. We use a simple

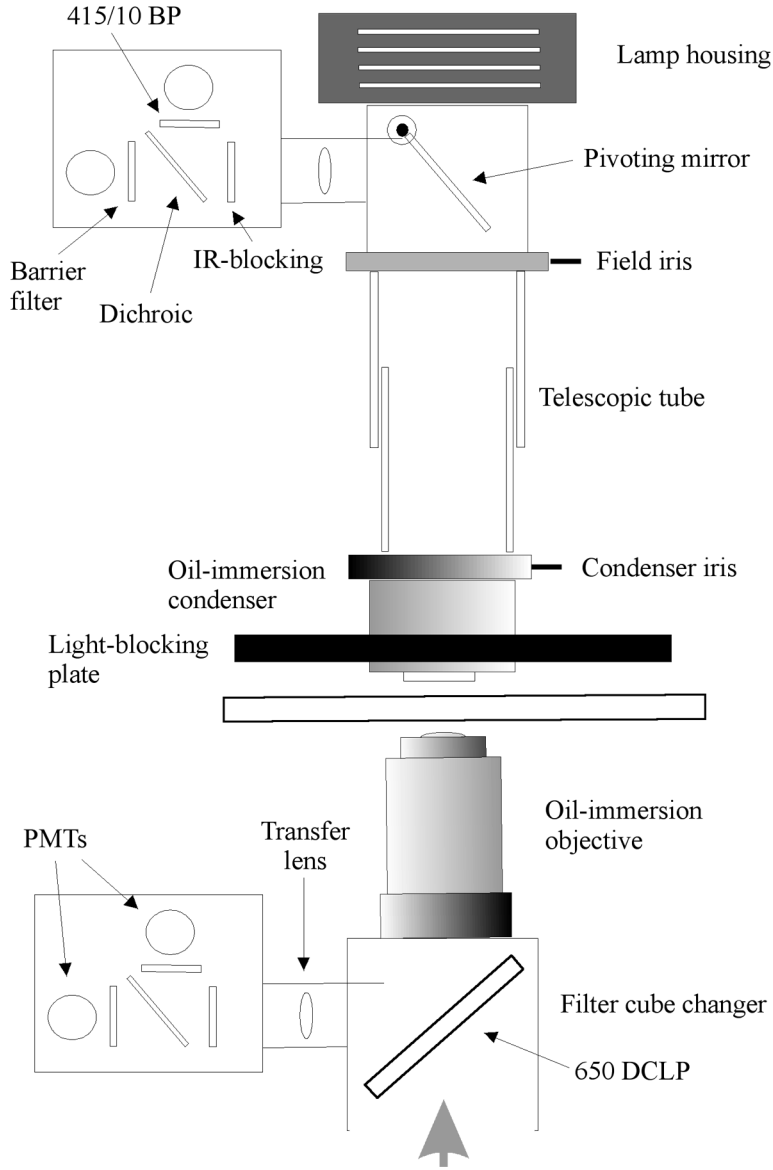


Fig. 1. Schematic arrangement of lens and detector arrangements on our Leica TCS2 MP/DMIRB inverted-microscope system. The two dual-channel detectors are identical and have removable filter cubes, so that different combinations are easy to assemble. The 650DCLP dichroic is mounted in a cube of the wide-field epifluorescence filter changer and directs all fluorescence returning through the objective to the detector. When this is rotated out of position, the normal confocal detection system can be used.

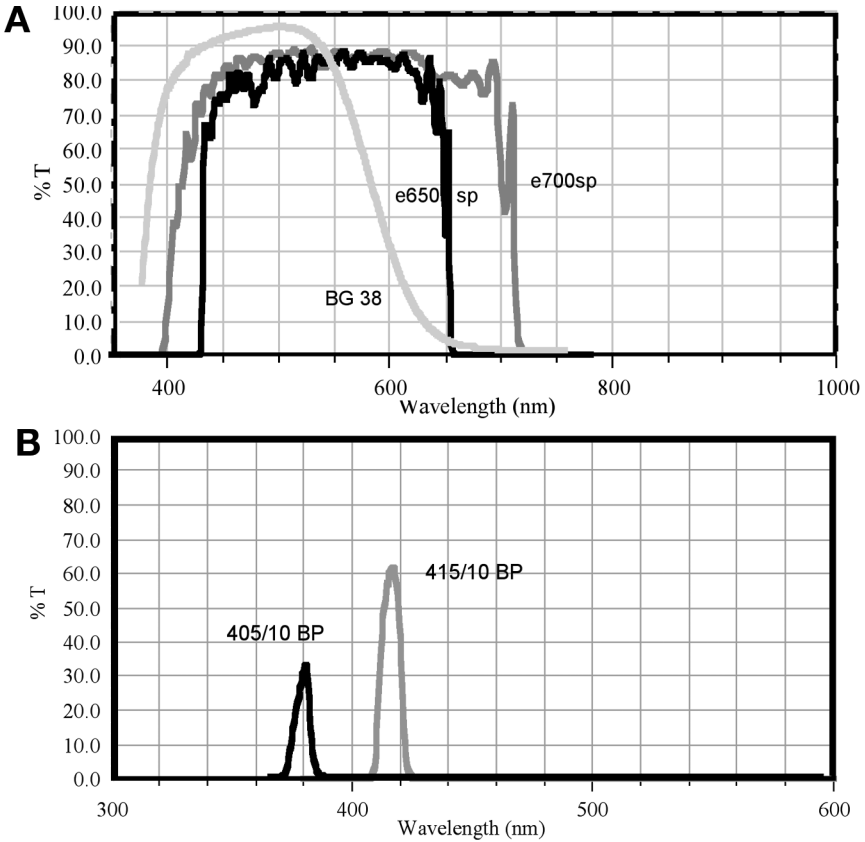


Fig. 2. (A) Curves of several infrared-blocking filters. The interference filters provide a sharp cutoff and good transmission. However, the e650 SP not only provides total blocking of the Ti-S laser light but also cuts off even the violet part of the visible spectrum. The e700 SP provides all of the visible spectrum but still cuts off at 400 nm and will also allow some laser light through at the short end of the tuning range. The colored glass filter BG38 is obviously very imperfect, allowing some leakage from 750 nm on and severely attenuating the red part of the visible spectrum; nevertheless, it transmits 80% at 400 nm and a usable fraction a little further into the ultraviolet. (B) Curves of two narrow-band filters suitable for detecting SHG signals. Because of the absorbance of the coating materials, only approx 35% transmission is attainable at 405 nm, so it will be preferable to tune the laser to 830 nm and use the 415-nm filter, which passes more than 60%. All spectra are reproduced by kind permission of Chroma Technology Corp.

aluminum disk, painted matt black, mounted in a filter holder, which will slip into one of the ventilation slots in front of the housing.

Filters for SHG detection need some careful consideration. As **Fig. 2A** shows, most infrared-blocking filters (essential to block transmitted laser light)

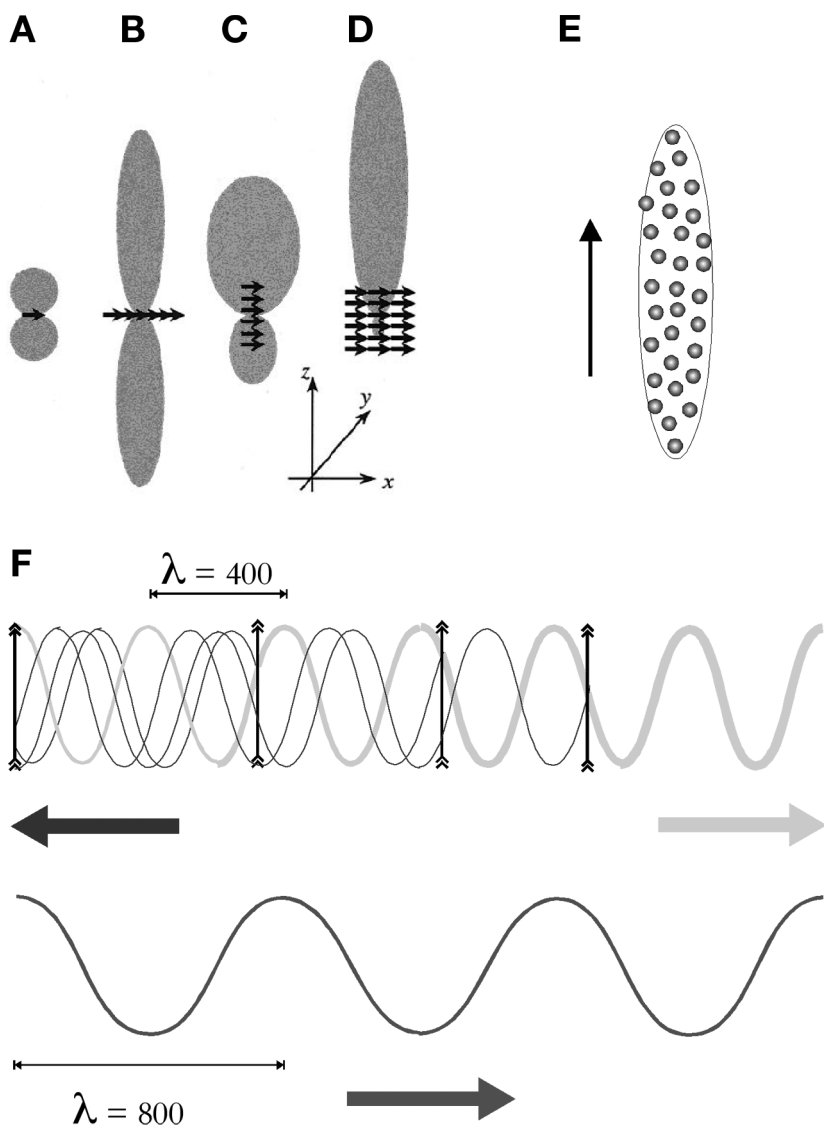


Fig. 3. Patterns of radiation from (A) single dipole, (B) array normal to the incident beam, (C) array in line with the incident beam, and (D) a bulk array. (D, from **ref. 18** by permission of the authors and *The Biophysical Society*). (E) Shape of the excitation point-spread function (psf) superimposed on typical collagen spacing in connective tissue. (A–D, from **ref. 12** with permission from Elsevier). (F) Randomly spaced fibers will propagate the second harmonic in a forward direction. Lower (red) wave is the excitation beam at 800 nm, propagating in the direction of the red arrow. The upper row shows second-harmonic radiation generated by the randomly spaced dipoles indicated by vertical arrows. Light propagated in the forward direction will be in step both with

also block light shorter than 400 nm. Therefore, even though most lasers can be tuned to wavelengths shorter than 800 nm, it will not be easy to detect the SHG signals in this part of the spectrum. Furthermore, the coatings used in most interference filters start to have strong absorption at wavelengths shorter than about 420 nm. At 415 nm, a 10-nm bandpass filter will transmit about 60% at its peak; at 405 nm, the equivalent filter will only transmit 30% (see **Fig. 2B**). Therefore, other things being equal, it is best to use an excitation wavelength of 830 nm or longer. We normally use 830-nm excitation and a 415-nm barrier filter.

3. Methods

3.1. Signal Propagation and Properties

Typically, depending on the extent to which the sample scatters light, between 80% and 90% of the SHG signal from collagen in a tissue sample will be propagated forward (**12**). **Figure 3** shows the direction of propagation of the signal from dipoles that are small compared to the wavelength propagated. Parts A–D were drawn to represent coherent anti-Stokes Raman scattering (CARS) microscopy (**18**) but are equally applicable to SHG. A single dipole (**Fig. 3A**) radiates in all directions *except* normal to the incident beam. A single, 40- to 50-nm collagen fiber would be expected to behave in this way. A planar array normal to the incident beam will radiate strongly forward and backward, because waves in both of these directions will be in phase (**Fig. 3B**). There will be little lateral propagation because in this direction, the wave from one dipole will not be in phase with the wave from its neighbor. An array orientated along the direction of the beam (**Fig. 3C**) will propagate strongly forward, because, regardless of the actual spacing (and even if it is completely irregular), all dipoles will have the same phase relationship to the exciting beam in the forward direction but will be randomly out of phase in the reverse direction (**Fig. 3F**). This same effect will be even more marked in a bulk array of dipoles (**Fig. 3D**), which will propagate the harmonic virtually exclusively forward. In SHG microscopy, the excited volume is elliptical, with the long axis along the direction of the beam, so that in any grouping of collagen fibers, there will be more excited dipoles in line with the beam than across it (**Fig. 3E**). Thus, whereas an isolated individual fiber may radiate its signal both forward and backward, overall the signal is predominantly propagated forward. In experiments with cryo-sections of human endometrium, we have found that only

Fig. 3. (*Continued*) the exciting radiation and light from other dipoles, whereas in the reverse direction, radiation from each dipole will have a random phase relation with any other, so little propagation will take place.

10–12% of the detectable SHG signal is propagated back through the objective lens (12), the remainder passing through the condenser to the transmitted light detector.

Although SHG uses long wavelengths, the resolution achievable is quite respectable. Calculated resolution values at 830 nm are around 250 nm (19), and measurements close to that have been reported in practice (12,16,19). **Figure 5C** shows resolution of this order in a histological section of skin. The depth resolution will be identical to that of TPF, and under best conditions, around 800 nm should be achieved. This is more than adequate for effective three-dimensional reconstructions (see **Fig. 6**).

3.2. Signal Detection and Imaging

3.2.1. Suitable Samples

The SHG signal from type I collagen is very strong—typically stronger than most two-photon excited fluorescence in biological samples—so that low excitation levels can be used. When fluorescence is being detected at the same time, the laser intensity needed will generally be determined by the fluorescent signal. SHG from collagen seems to be unaffected by most preparation techniques. Good images can be obtained from histological paraffin sections, whether unstained (see **Fig. 4**) or stained with routine histological stains such as hematoxylin and eosin or Masson's trichrome (**Figs. 5,6; refs. 12,16**).

Sirius Red, which stains collagen and also enhances its birefringence (20,21), also has no effect on the SHG, although it is noticeable that the second-harmonic signal does not exactly colocalize with two-photon excited fluorescence from Sirius Red (12) or with the autofluorescence from aldehyde-fixed collagen (see **Fig. 4**). We have suggested that only the highly crystalline collagen gives the SHG signal and stains (and aldehydes) have more effect on surrounding less crystalline material; colocalization analyses support this (22).

One common preparation technique does seem to compromise the SHG signal from collagen. It is severely depleted in epoxy resin-embedded blocks of tissue fixed in glutaraldehyde and osmium tetroxide for electron microscopy, even when sectioned at 500 nm thickness for the optical microscope. Even though some signal is still present, on the basis of our preliminary trials we cannot recommend this material for SHG imaging; a disappointing conclusion for those needing to combine optical and electron microscope imaging of collagen.

The image formation in three dimensions is effectively equivalent to that in multiphoton fluorescence; therefore depth penetration in turbid and scattering samples will be substantially better than in single-photon confocal microscopy, the predominantly forward propagation of the signal does impose some restrictions on sample thickness for optimal imaging. Whereas in multiphoton mode one can simply probe down into a thick specimen until the point of no signal is

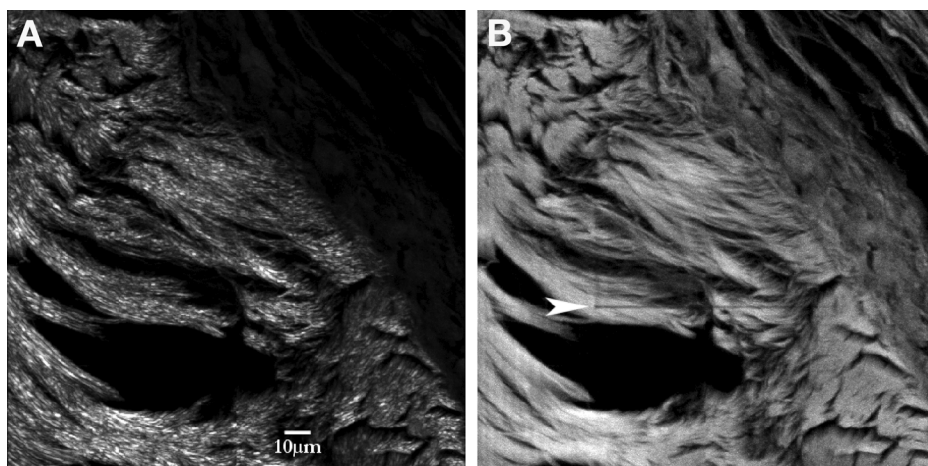


Fig. 4. Micrographs of kangaroo-tail tendon transplanted into rat muscle. Projection from 24 optical sections. Aldehyde-fixed, unstained paraffin section cleared in xylene and permanently mounted. For more details of the sample, *see refs. 12 and 18*. The implanted tendon is seen in the lower left half of the picture, and the host tissue (including some type III collagen from the host response) is seen in the upper right. **(A)** Forward-propagated signal, almost exclusively SHG at 410 nm, although detected over a wide spectral range (400–550 nm). **(B)** Back-propagated signal in the spectral range 500- to 550-nm showing aldehyde-induced autofluorescence. The photomultiplier tube voltage was set 100 V higher than in **(A)** in order to pick up the much weaker autofluorescence. Previous collection of an image at a higher zoom setting has caused slight bleaching in the fluorescent image (arrowed), but the second-harmonic image is unaffected. Note that no SHG signal is visible in the type III collagen (upper right), implying that if it either produces no, SHG signal or a much weaker, SHG signal.

reached, for optimal imaging in SHG microscopy the signal has to be able to pass through the entire sample. Thus, in either case, the penetration depth might be 200 μm ; however, in SHG, the sample itself cannot be too much thicker than this. With thicker samples, one often can image down to a considerable depth at the edge of the specimen when no signal can be detected in the center—a consequence of the large angle through which the signal is generated and propagated. Alternatively, one can simply use the backscattered image; even though up to 90% of the signal might be lost, in a suitable sample it might still be possible to collect a good image (23).

3.2.2. Detection Strategies

Because the SH signal is by definition shorter than any two-photon excited fluorescence, a 10-nm FWHM filter will completely exclude any fluorescent signal. **Figure 6** shows SH images collected in this way. Although this does

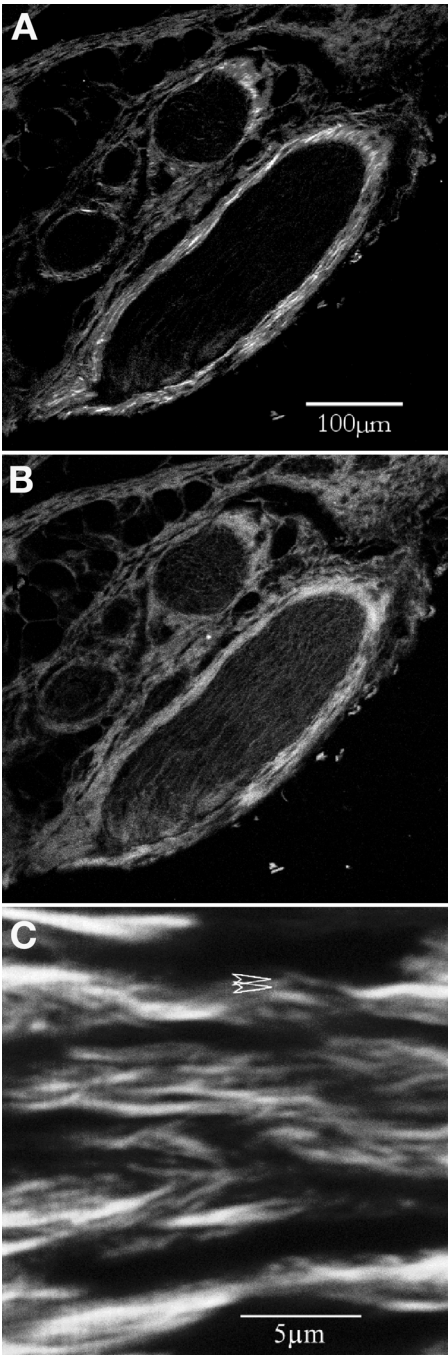


Fig. 5. Histological paraffin section of skin, stained with Masson's trichrome. (A) and (B) taken with 20× NA 0.5 lens, using 800-nm excitation and a broad-band collection

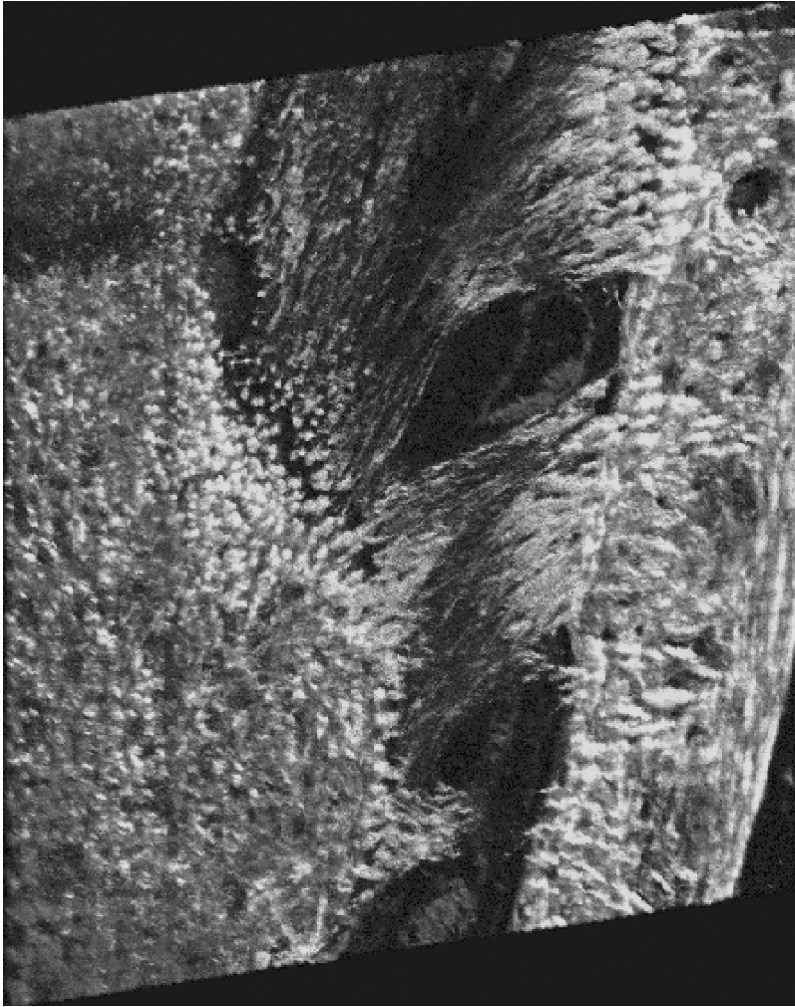


Fig. 6. Rendered image (simulated fluorescence projection at an oblique angle) from 20 optical sections through a histological section of the periodontal membrane of a developing tooth. SHG image, showing collagen only, captured with BP 415/10 filter, 25 \times NA 0.75 oil-immersion objective, 830-nm excitation.

Fig. 5. (*Continued*) filter. (A) Transmitted image; (B) back-propagated image of collagen around hair follicles in mouse skin. (A) shows both fluorescence and SHG, but the SHG is substantially brighter and is easily recognisable without any formal separation. (C) High-power image ($\times 100$ NA 1.4 objective) taken using 830-nm excitation and a BP 415/10 filter (Fig. 2) to exclude all fluorescence. Only collagen is seen and the resolution is excellent (arrowheads are spaced 330 nm apart).

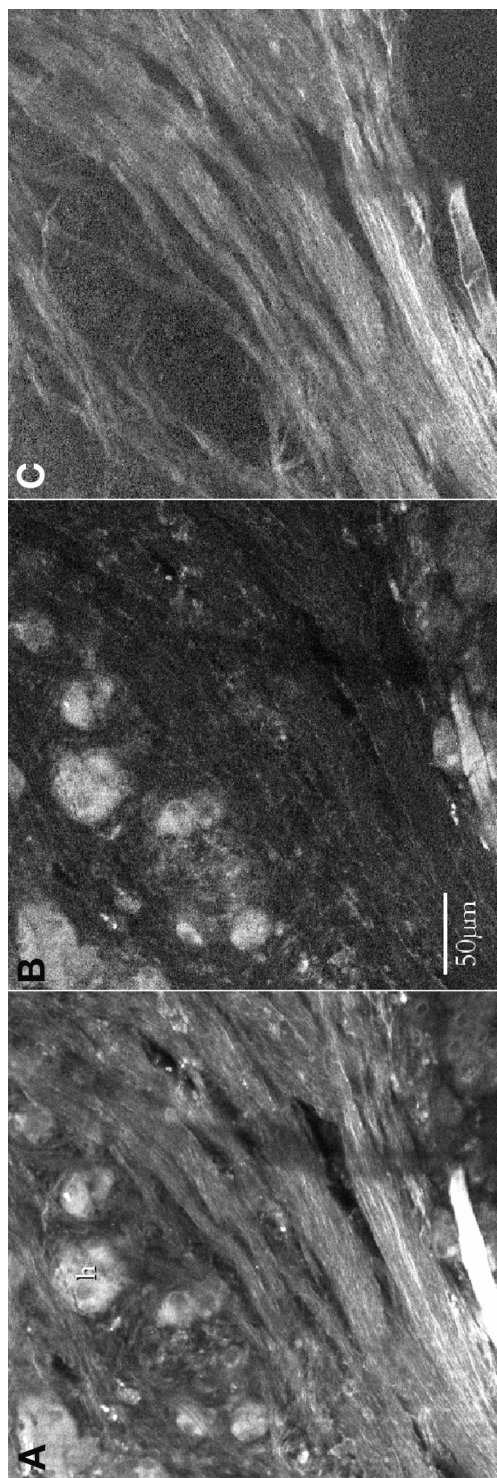


Fig. 7. Separation of signals by image subtraction, human cirrhotic liver biopsy. (A) Signal collected between 400 and 560 nm in the transmission detector, containing SHG and fluorescence. (B) Signal collected between 500 and 560 nm in the back-propagated nonde-canned detector, showing only fluorescence. (C) Image B scaled to match intensities on the hepatocytes (h) and subtracted from image A, giving an image that shows only the SHG signal.

make detection absolutely unambiguous, it restricts excitation to wavelengths for which the appropriate filter is available.

Sometimes excitation of other fluorochromes makes it desirable to tune the laser to wavelengths for which the user does not have a suitable filter or for which a good filter is unavailable (such as close to 800 nm to excite DAPI or Hoechst). Also, a researcher wishing to find out whether SHG imaging can be useful in a particular project will probably not want to purchase special filters initially.

Fortunately, the fact that the wavelength must always be shorter than that of any two-photon excited fluorescence (as fluorescence always involves a Stokes shift) means that it is often quite easy to distinguish an SHG signal without custom filters. This is particularly handy for those cases in which one is not looking at the SHG signal in isolation. Often, an experiment will require one or more fluorochromes to be imaged in the same sample. Because the SHG signal from collagen can be excited anywhere within the tunable range of a Ti-S laser, it is often desirable to optimize the excitation for the fluorochrome rather than having the collagen signal at the wavelength of a particular bandpass filter. Particularly if there is not much autofluorescence (which tends to have a broad spectrum) present, one might be able to use the shorter wavelength of the collagen signal to distinguish it with nothing more than a conventional short-pass/dichroic/long-pass combination. For example, in a specimen stained with routine fluorochromes (FITC, TRITC, etc., without DAPI), there will be very little fluorescence (even autofluorescence) shorter than 500 nm, so a 500 DCLP dichroic in the detector will give a signal that is predominantly SHG in the short-wavelength channel. **Figure 4** shows an example of this; even with a 560 nm dichroic, the short part of the spectrum is totally dominated by the SHG signal while a strong fluorescent signal is detected in the range 560–650 nm. (In this sample, which is unstained, this is partly a function of the strength of the SHG signal from the highly crystalline kangaroo-tail collagen and partly a reflection if the aldehyde-induced autofluorescence tends to peak around 580 nm).

Where fluorescence is stronger in the short wavelengths, so that this strategy will not work, it is simple to use the directionality of the SHG signal to detect it, because fluorescence will propagate equally in all directions. If matching filters are used, the transmitted detector will show a combination of fluorescence and SHG signals (**Fig. 5A**), whereas back-propagated detectors (see **Fig. 1**), whether confocal or nondescanned, will show mostly or entirely fluorescence (**Fig. 5B**). Therefore, subtracting the “reflected” signal from the “transmitted” signal will leave only the SHG signal. **Figure 7** shows an example of this. The sample is a cirrhotic liver, which has a very high level of autofluorescence. Cirrhosis (fibrosis) of the liver is a proliferation of collagen fibers through the liver, and SHG microscopy is proving to be a powerful tool

to study it (*12,23*). The transmitted detector collects both SHG and fluorescent signals (*see Fig. 7A*), whereas the back-propagated signal has only the fluorescence (*see Fig. 7B*). The simple procedure to isolate the SH signal can be done in any image analysis or image processing program. The steps are as follows:

1. Measure intensity in both images of an area known to show only fluorescence (in this example, the hepatocytes labeled h).
2. Scale the intensity of the fluorescence-only image (**Fig. 7B**) so that it matches the corresponding area in the combined image (**Fig. 7A**). In this case, the image in **Fig. 7B** needs to be scaled up by approx 10%.
3. Subtract the image, in **Fig. 7B** from the image in **Fig. 7A**. The resulting image (**Fig. 7C**) shows only the SHG signal.

The two-color combination of this SHG-only image with the fluorescence-only image can be seen as Fig. 7B of **ref. 12**.

In principle, one could also use fluorescent lifetime to separate the SH signal from fluorescence, although this does not seem to have been done in practice. Generation of the SH signal is virtually instantaneous, whereas, typically, fluorescence does not appear for several hundred picoseconds and then decays over 3–12 ns. With a suitably high time resolution, the signals should therefore be quite distinct.

3.3. Conclusion: Applications for SHG Imaging of Collagen

Although the ability of collagen to excite second harmonics has been known for 20 yr (*10*), and putative uses for the technique have been proposed as long as 16 yr ago (*13*), it has only been in the past 2 yr that advances in microscope and laser technology have brought SHG microscopy at high resolution into the hands of histologists and cell biologists. At this stage, it might be premature to predict what its final use will be.

Two broad areas seem likely: the use of SHG imaging as a tool to study the three-dimensional architecture of collagen in fine detail at the microscopic level in both healthy and diseased tissue, and its use to investigate changes in collagen in disease. On the former front, SHG has already been used to study the arrangement of collagen in human endometrium as part of a long-term study of the glandular and vascular structure in three dimensions (*12,16,24*). It is also being developed as a method for detecting and quantifying collagen invasion in cirrhotic liver (*12,25*).

We have shown (*12*) that SHG imaging appears to be able to distinguish between at least some collagen types (*see Fig. 4*). Current research in our laboratory aims to quantify and characterize this by using pure and well-defined collagen samples (*22*). SHG has also been used as a tool to detect the polarity of collagen in connective tissue (*13*) and this might also become applicable at higher resolution with current developments in instrumentation. Experimentally

induced damage has been shown to affect the SH signal from collagen (**14**) and, very recently, pathologic changes have also been shown to be detectable by the SHG properties (**15**). Teeth have a well-characterized collagen structure, and the SH signal is detectable in sectioned tooth material with and without decalcification (*see Fig. 6*). A study is currently in progress using SHG to study changes in collagen associated with dental caries.

Hereditary collagen diseases are another area, as yet unexplored, in which SHG imaging could have a significant impact. Now that multiphoton microscopes are in wide use, it seems inescapable that the associated technique of SHG microscopy will grow steadily more important in future years.

4. Notes

1. The process of second harmonic generation (SHG) has been summarized in a recent paper by Gauderon et al. (**2**). Briefly, as electromagnetic radiation propagates through matter, the electric field (E) exerts forces on the sample's internal charge distribution. The consequent redistribution of charge generates an additional field component. The resultant dipole moment per unit volume is referred to as the electric polarization (P) and can be expressed as a sum of linear and nonlinear terms. The nonlinear components only become significant at very high light intensities. The primary nonlinear effect is a polarization of second order in the electric field and is given by (**27**)

$$P_i^{2\omega} = \chi_{ijk}^{2\omega} E_j^{\omega} E_k^{\omega} \quad (1)$$

where subscripts denote Cartesian components and superscripts denote the relevant frequencies. χ is a ($3 \times 3 \times 3$) third-rank tensor, termed the second-order nonlinear optical susceptibility, whose elements sum to zero for material with inversion symmetry.

2. In 1974, Hellwarth and Christiansen (**3**) looked at crystals illuminated by focused laser light in a conventional wide-field microscope. This is not an effective use of the nonlinear imaging properties of SHG; it is not depth-selective and the photon flux required to excite the entire visible field at the same time is extreme. Further, the difficulty of excluding exciting light from the image is considerable. It is, therefore, not a practically useful technique, although it does have the advantage, compared to scanning techniques, that the wavelength of the emitted light (the second harmonic) determines the resolution.
3. "Prechirping" (i.e., retarding the shorter wavelengths before the pulse enters the fiber) has been used to compensate for this but has the practical inconvenience that the "prechirp" must be adjusted for different wavelengths and pulse lengths. This, in turn, is likely to mean realigning the beam entering the microscope. Changing wavelengths—one of the key merits of the Ti-S laser—is thus made difficult and tedious; therefore, this solution has not gained general acceptance.
4. Two-photon excitation maxima for common members of the Clontech GFP family are as follows: eCFP = 860 nm, eGFP = 920 nm, eYFP = 960 nm, Ds-Red = approx 975 nm (**17**).

Acknowledgments

We are very grateful to Allan Jones, Frank Manconi, Anne Swan, and Mark Gorrell for samples, discussion, and collaboration. We also owe a deep debt to Colin Sheppard for introducing us to second-harmonic microscopy, and to Régis Gauderon and Paul Xu for working to develop and evaluate the technique. The microscope was purchased through a Research Infrastructure (Equipment and Facilities) grant from the Australian Research Council. We thank Sunney Xie and colleagues, the *Biophysical Journal*, and the Biophysical Society for allowing us to reproduce Fig. 3 A–D, and the *Journal of Structural Biology* for allowing us to reproduce Fig. 3E. We likewise thank Chroma Technology Corp. for permission to reproduce the filter curves shown in Fig. 2. We are very grateful to José Feijó for critically reading and substantially improving the final manuscript.

References

1. Franken, P. A., Hill, A. E., Peters, C. W., and Weinreich, G. (1961) Generation of optical harmonics. *Phys. Rev. Lett.* **7**, 118–119.
2. Gauderon, R., Lukins, P. B., and Sheppard, C. J. R. (2001) Simultaneous multi-channel nonlinear imaging: combined two-photon excited fluorescence and second harmonic generation microscopy. *Micron* **32**, 685–689.
3. Hellwarth, R. and Christensen, P. (1974) Nonlinear microscopic examination of structure in polycrystalline ZnSe. *Opt. Commun.* **12**, 318–322.
4. Gannaway, J. N. and Sheppard, C. J. R. (1978) Second harmonic imaging in the scanning optical microscope. *Opt. Quant. Electron.* **10**, 435.
5. Campagnola, P., Clark, H. A., Mohler, W. A., Lewis, A., and Loew, L. M. (2001) Second-harmonic imaging of living cells. *J. Biomed. Opt.* **6**, 277–286.
6. Campagnola, P. J., Millard, A. C., Terasaki, M., Hoppe, P. E., Malone, C. J., and Mohler, W. A. (2002) Three-dimensional high-resolution second-harmonic generation imaging of endogenous structural proteins in biological tissues. *Biophys. J.* **81**, 493–508.
7. Mertz, J. and Moreaux, L. (2001) Multi-harmonic light microscopy: theory and applications to membrane imaging, in *Multiphoton Microscopy in the Biomedical Sciences* (A. Periasamy and P.T.C. So, eds.), *Proceedings of SPIE* **4262**, 9–17.
8. Moreaux, L., Sandre, O., Charpak, S., Blanchard-Desce, M., and Mertz, J. (2001) Coherent scattering in multi-harmonic microscopy. *Biophys. J.* **80**, 1568–1574.
9. Lodish, H., Berk, A., Lipursky, S. L., Matsudaira, P., Baltimore, D., and Darrell, J. (2000) *Molecular Cell Biology*, 4th ed., W. H. Freeman, New York.
10. Roth, S. and Freund, I. (1981) Optical second-harmonic scattering in rat-tail tendon. *Biopolymers* **20**, 1271–1290.
11. Georgiou, E., Theodossiou, T., Hovhannisya, V., Politopoulos, K., Rapti, G. S., and Yova, D. (2000) Second and third optical harmonic generation in type I collagen, by nanosecond laser irradiation, over a broad spectral region. *Opt. Commun.* **176**, 253–260.

12. Cox, G., Kable, E., Jones, A., Fraser, I., Manconi, F., and Gorrell, M. (2002) 3-dimensional imaging of collagen using second harmonic generation. *J. Struct. Biol.* **141**, 53–62.
13. Freund, I., Deutsch, M., and Sprecher, A. (1986) Connective tissue polarity. Optical second-harmonic microscopy, crossed-beam summation, and small-angle scattering in rat-tail tendon. *Biophys. J.* **50**, 693–712.
14. Kim, B. M., Eichler, J., Reiser, K. M., Rubenchik, A. M., and Da Silva, L. B. (2000) Collagen structure and nonlinear susceptibility: effects of heat, glycation, and enzymatic cleavage on second harmonic signal intensity. *Lasers Surg. Med.* **27**, 329–335.
15. Deng, X., Williams, E. D., Thompson, E. W., Gan, X., and Gu, M. (2002) Second harmonic generation from biological tissues: effect of excitation wavelength. *Scanning* **24**, 175–178.
16. Cox, G. C., Manconi, F., and Kable, E. (2002) Second harmonic imaging of collagen in mammalian tissue. *Proc. SPIE* **4620**, 148–156.
17. Blab, G. A., Lommerse, P. H. M., Cognet, L., Harms, G. S., and Schmidt, T. (2001) Two-photon excitation action cross-sections of the autofluorescent proteins. *Chem. Phys. Lett.* **350**, 71–77.
18. Ji-Xin Cheng, Kevin Jia, Y., Gengfeng Zheng, and Sunney Xie, X. (2002) Laser-scanning coherent anti-Stokes Raman scattering microscopy and applications to cell biology. *Biophys. J.* **83**, 502–509.
19. Cox, G., Kable, E., Sheppard, C. J. R., and Xu, P. (2002) Resolution of second harmonic generation microscopy. Durban, South Africa. *Proc. 15th Int. Cong. Electron Microscopy* **2**, 331–332.
20. Schräpler, V. R., Schmidt, T., Schultka, R., and Hepp, W-D. (1991) Farbstoffanalytische Untersuchungen zum polarisationsmikroskopischen Nachweis von Kollagen mit Solaminrot 4B (Teil II). *Acta Histochem.* **90**, 75–85.
21. Milthorpe, B. K. (1994) Xenografts for tendon and ligament repair. *Biomaterials* **15**, 745–752.
22. Cox, G. C., Xu, P., Sheppard, C. J. R., and Ramshaw, J. (2003) Characterization of the second harmonic signal from collagen. *Proceedings of SPIE* **4963**, 32–40.
23. Zipfel, W. R., Williams, R. M., Christie, R., Nitikin, A. Y., Hyman, B. T., and Webb, W. W. (2003) Live tissue intrinsic emission microscopy using multiphoton excited native fluorescence and second harmonic generation. *Proc. Natl. Acad. Sci. USA* **100**, 7075–7080.
24. Manconi, F., Cox, G., Kable, E., Markham R., and Fraser, I. S. (2001) Computer-generated three-dimensional reconstruction of uterine histological parallel serial sections displaying microvascular and glandular structures in human endometrium. *Micron* **32**, 449–453.
25. Gorrell, M. D., Wang, X. M., Levy, M. T., et al. (2003) Intrahepatic expression of collagen and fibroblast activation protein (FAP) in hepatitis c virus infection. *Adv. Exp. Med. Biol.* **524**, 235–243.
26. Yariv, A. (1967) *Quantum Electronics*, Wiley, New York.



<http://www.springer.com/978-1-58829-157-8>

Cell Imaging Techniques

Taatjes, D.J.; Mossman, B.T. (Eds.)

2006, XIV, 490 p. 212 illus., Hardcover

ISBN: 978-1-58829-157-8

A product of Humana Press